scientific reports

OPEN

Climate-driven dust intensification over the Mongolian Gobi in early spring

Sang-Seok Oh[1], Husile Bai[2], Hyo-Jung Lee[1,3]✉, Hyun-Young Jo[4] & Cheol-Hee Kim[1,3]✉

While dust activation has declined across most of East Asia over recent decades, springtime dust storms have intensified over the Mongolian Gobi, suggesting a regionally distinct response to climate change. This study focuses on March, the early stage of the dust season, when snow cover and land–atmosphere interactions are particularly sensitive to climatic conditions. Using 24 years (2000–2023) of multi-platform observations and ERA5 reanalysis, we show that increasing surface susceptibility driven by snow loss and soil drying coincides in early spring with persistent baroclinic instability and sustained upper-level thermal winds over this region. These atmospheric conditions, which are absent over neighboring dust source areas, prevent the dynamical weakening typically associated with mid-latitude warming. In contrast, over the Loess Plateau, reduced thermal winds act as a compensating response that suppresses dust mobilization despite surface drying. As a result, the Mongolian Gobi experiences an unmitigated climate penalty, where both land-surface drying and persistent atmospheric circulation jointly amplify dust emissions under ongoing warming. Our findings reveal how regional climate dynamics can fundamentally reshape dust-source activation in early spring across East Asia under a warming climate.

Keywords Mongolian Gobi, Dust, Baroclinic instability, Snow cover

Dust storms are natural atmospheric phenomena with profound ecological, climatic, and socio-economic consequences[1,2]. In arid and semi-arid regions, these storms mobilize large quantities of mineral particles that can travel long distances, affecting air quality, ecosystem health, and human well-being far beyond their origins[3–5]. Although dust activation has generally declined across many East Asian deserts in recent decades[6–9], the Mongolian Gobi, one of the largest dust source regions in Northeast Asia[2,10–13], has experienced a pronounced intensification of early-springtime (particularly March) dust storms under ongoing climate warming (Fig. 1). The region has undergone rapid surface warming[14], changes in precipitation regimes[15–17], and substantial snow cover loss[18], all of which accelerate soil drying and increase the land surface's susceptibility to wind erosion[19]. These warming-induced surface changes impose a climate penalty, defined here as an amplification of land-surface susceptibility to dust emission under a warming climate. Here, "surface susceptibility" refers to the set of land-surface conditions (e.g., reduced snow cover, decreased soil moisture, and increased soil temperature) that enhance the erodibility of the surface and favor dust emission. However, the atmospheric dynamical processes governing whether this surface penalty is amplified or mitigated remain poorly understood.

Climate-induced Arctic amplification has weakened the meridional temperature gradient, leading to reduced baroclinicity and weakened upper-level thermal winds across much of the mid-latitudes[20]. This dynamical response suppresses vertical wind shear and mechanical turbulence, partially offsetting the enhanced surface susceptibility associated with warming. Such compensating effects have contributed to the observed decline in dust activation over regions such as the Loess Plateau, where increased vegetation cover and weakened winds jointly limit dust mobilization[6,7](Fig. S1).

However, the mid-latitude atmospheric response to climate change is not spatially uniform. Instead, it reflects a climatic tug-of-war between Arctic amplification and subtropical warming. While Arctic warming tends to weaken the jet stream and suppress baroclinic activity, subtropical warming can intensify upper-level thermal winds and enhance wave activity[20,21]. The Mongolian Gobi represents a distinct manifestation of this competition. In recent decades, persistent baroclinic instability and sustained upper-level thermal winds over

[1]Department of Atmospheric Sciences, Pusan National University, Busan 46241, Republic of Korea. [2]Department of Earth and Environmental Sciences, Vanderbilt University, 2201 West End Ave, Nashville, TN 37235, USA. [3]Institute of Environmental Studies, Pusan National University, Busan 46241, Republic of Korea. [4]Changwon Research Institute, Changwon 51500, Republic of Korea. ✉email: hyojung@pusan.ac.kr; chkim2@pusan.ac.kr

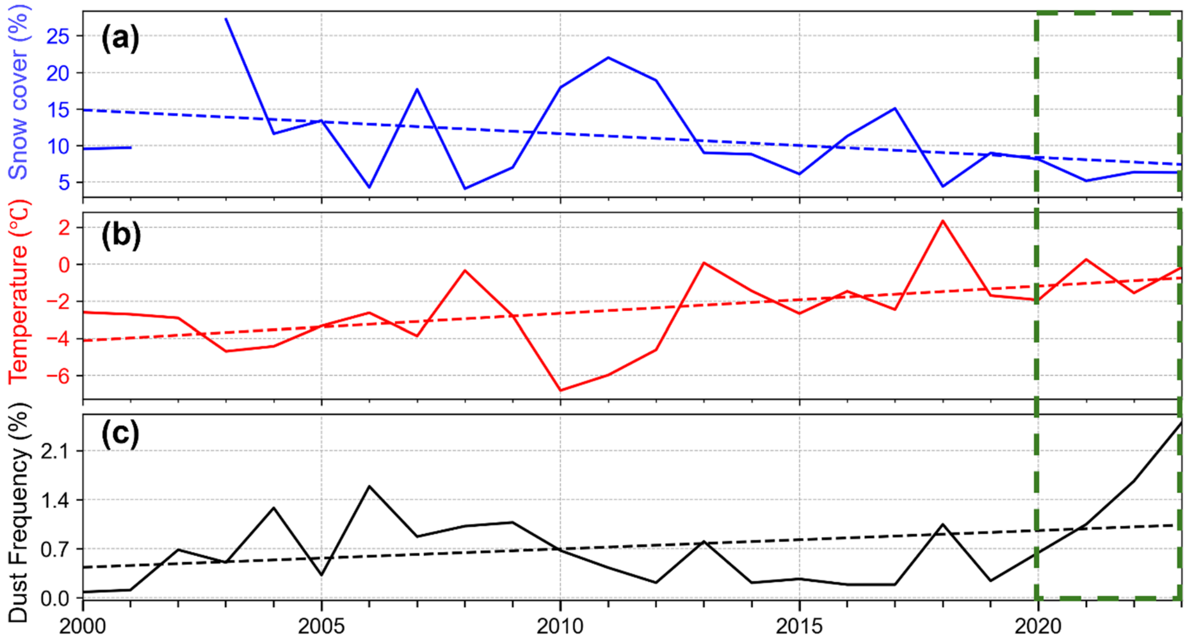

Fig. 1. Time series over 24 years (2000 – 2023) of (a) snow cover (blue line) averaged over the Mongolian Gobi using Terra-Modis data, (b) 2 m air temperature variations (red line) averaged over the same Mongolian Gobi from ERA5, and (c) dust occurrence frequency (black line) from SYNOP observations at 15 sites.

this region have amplified rather than mitigated the surface climate penalty associated with snow loss and soil drying. As a result, the region remains highly vulnerable to the combined effects of atmospheric instability and land-surface aridification.

Although large-scale atmospheric dynamics are known to influence dust activation, most previous studies have focused primarily on surface conditions or phenomenological descriptions of dust events. The roles of springtime baroclinic instability and persistent upper-level winds in regulating dust emissions have not been systematically quantified. Here, we develop a framework that explicitly links upper-level atmospheric circulation to surface dust mobilization, demonstrating how large-scale atmospheric dynamics act together with land-surface drying to produce a compound climate penalty on dust activation.

Using Surface Synoptic Observation (SYNOP), Terra Moderate Resolution Imaging Spectroradiometer (MODIS) satellite retrievals, and ECMWF Reanalysis v5 (ERA5) from 2000 to 2023, we examine the coupled roles of surface conditions and atmospheric dynamics in driving March dust outbreaks over the Mongolian Gobi. March represents the early stage of the East Asian dust season, when rapidly changing surface conditions allow land–atmosphere coupling to strongly influence dust activation. This seasonal distinction reflects differences in dominant controlling mechanisms between March and later spring months (April–May). Our results identify this region as a climate-sensitive dust hotspot, where the interaction between persistent upper-level circulation and progressive surface drying fundamentally reshapes dust-source behavior under continued warming.

Results and discussion

The Mongolian Gobi is warming rapidly, with an annual mean temperature increasing by about 0.15 °C/year, one of the fastest rates of warming among East Asia's major dust source regions[22] (Fig. 1b) Notably, this warming is particularly pronounced during early spring, especially in March, a critical transitional period when snow cover, soil moisture, and surface wind conditions undergo rapid seasonal changes (Fig. 2). This study therefore focuses on March, when snow cover retreat and soil exposure strongly modulate surface susceptibility to wind erosion. During this early stage of the dust season, land–atmosphere coupling plays a particularly important role in determining whether atmospheric dynamical forcing can trigger dust activation. In contrast, dust activation later in spring (e.g., April) is more strongly influenced by large-scale circulation variability and synoptic weather systems affecting the Mongolian Gobi, including modes such as the Arctic Oscillation. The Mongolian Gobi typically retains substantial snow cover through March owing to its high-latitude location, which stabilizes the land surface by shielding soil and suppressing wind erosion (Fig. S2). Recent warming has driven a sharp decline in snow cover, particularly in central and northern areas, increasing the surface's susceptibility to wind erosion (Fig. 1). A strong positive correlation between snow cover and soil moisture ($r = 0.61$, $p < 0.1$) underscores the role of snowmelt in sustaining springtime surface stability[23]. Loss of snow cover also decreases surface albedo, amplifying local warming and accelerating soil evaporation (Fig. 2, Fig. S3). Together, these processes establish a positive feedback that intensifies surface desiccation and enhances dust-emission potential.

Dust activation has increased markedly since 2020, coinciding with warmer and drier surface conditions (Fig. 1, green dashed box). A spatial analysis confirmed widespread enhancement of dust activation across the Mongolian Gobi (Fig. S4). A significant negative correlation between snow cover and dust frequency ($r = -0.4$,

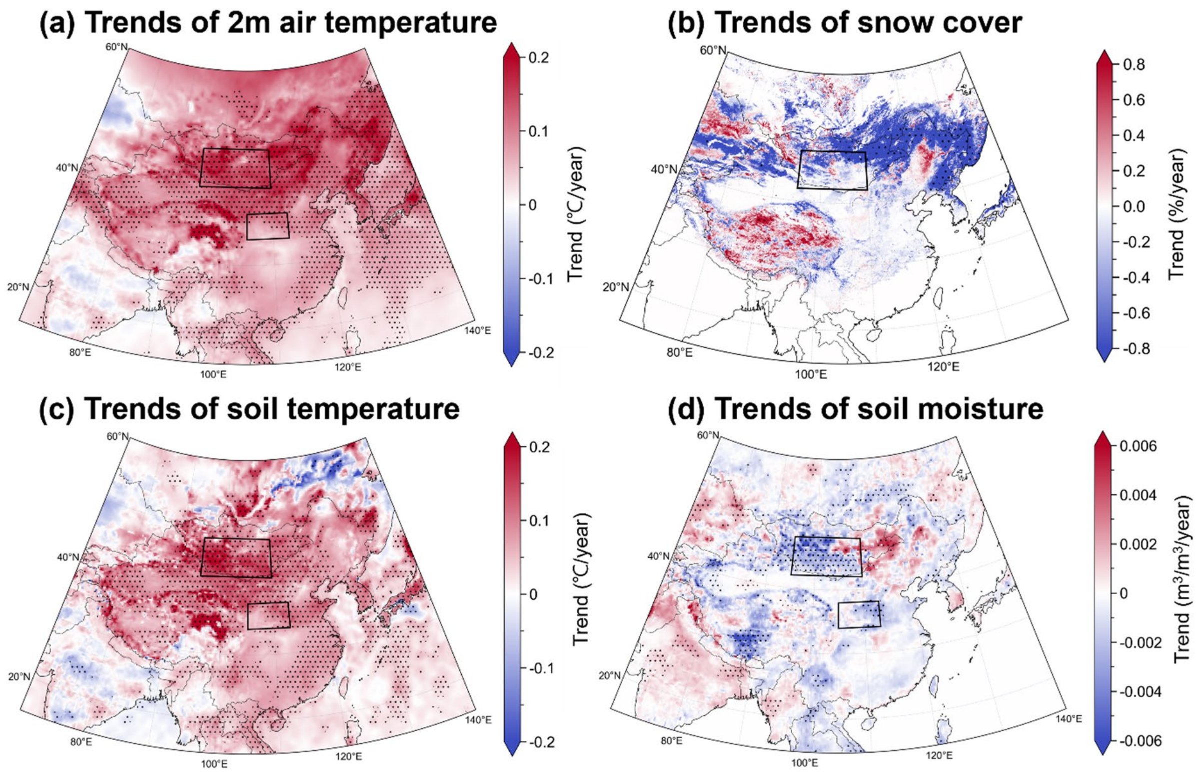

Fig. 2. Spatial distribution of linear trend in (**a**) 2 m air temperature (℃/year), (**b**) snow cover (%/year), (**c**) soil temperature (℃/year), and (**d**) soil moisture (m3 /m3 /year) over 24 years (2000 – 2023), respectively. Black dots indicate grid points where the trends are statistically significant ($p < 0.1$).

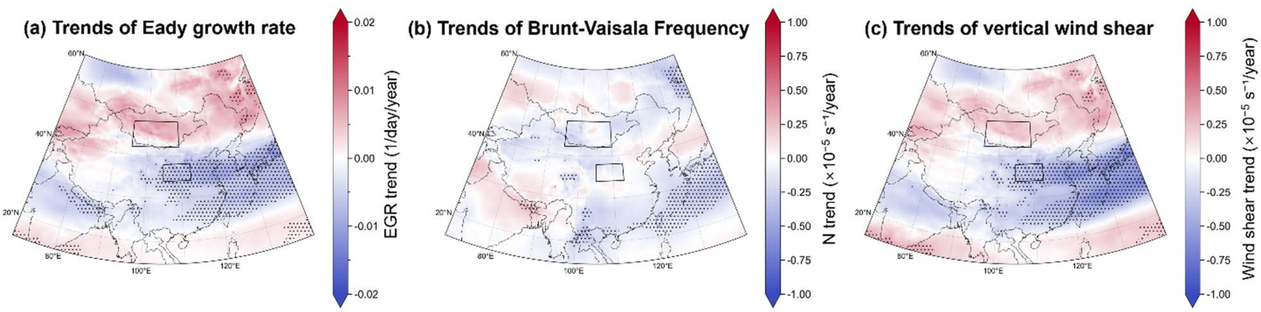

Fig. 3. Spatial distribution of the linear trend in March (2000–2023) of (**a**) the Eady Growth Rate (EGR), (**b**) the Brunt-Vaisala frequency (N), and (**c**) vertical wind shear between 850 and 500 hPa over East Asia. Trends are estimated using linear regression for each grid point. Dotted areas indicate regions where the trends are statistically significant at the 90% confidence level ($p < 0.1$). Rectangles denote the selected dust source regions analyzed in this study.

$p < 0.1$) further supports the role of snow-cover loss in driving dust mobilization (Fig. S5). However, snow-cover changes alone do not fully account for the abrupt surge in dust activation observed since 2020.

While rising temperatures and declining snow cover increase surface susceptibility to dust emissions, atmospheric dynamics provide the necessary triggering mechanism for dust uplift and transport[24–26]. Adequate wind intensity and atmospheric instability are required to initiate dust uplift and sustain long-range transport. Thus, thermal factors primarily establish dust-prone surface conditions, whereas dynamic factors such as wind speed and atmospheric instability control the actual release and movement of dust particles.

We quantified baroclinic instability using the Eady Growth Rate (EGR), which incorporates vertical wind shear and atmospheric stability[27]. The Loess Plateau exhibited a significant decreasing trend in March EGR from 2000 to 2023, whereas the Mongolian Gobi showed no such decline and instead exhibited an increasing trend (Fig. 3). This contrast indicates that, unlike the Loess Plateau, the Mongolian Gobi lacks a compensating atmospheric weakening that would otherwise suppress dust activation. Consequently, persistent baroclinic instability acts in concert with surface drying to intensify the compound climate penalty.

This finding distinguishes the Mongolian Gobi from other major dust source regions in East Asia and highlights the persistence of a unique dynamical environment in recent decades. The contrasting regional behavior can be understood by examining the two components of the EGR. In both the Mongolian Gobi and the Loess Plateau, a weakening tendency in the Brunt–Väisälä frequency (N) associated with lower-tropospheric heating was observed; however, this trend did not reach statistical significance over the full period from 2000 to 2023. Thermodynamic stabilization alone therefore cannot explain the divergent evolution of baroclinic instability between the two regions. Instead, the dominant difference arises from vertical wind shear. Over the Mongolian Gobi, vertical wind shear is not statistically significant, indicating the persistence of a baroclinic environment that continues to support strong synoptic-scale circulation (Figs. 3 and 4). In contrast, the Loess Plateau experienced a pronounced weakening of vertical wind shear, driven primarily by a substantial reduction in 500 hPa upper-level winds (Figs. S5, S6), associated with the decline in EGR. This pattern is consistent with the thermal wind relationship linking upper-level winds and vertical wind shear in baroclinic systems.

The weakening of upper-level winds over the Loess Plateau can be attributed to a reduction in the meridional gradient of 500 hPa geopotential height. Specifically, as shown in the latitudinal profile of temperature trends (Fig. S7), the warming rate increases sharply with latitude up to approximately 45°N. For Loess Plateau (located south of this peak), this northward-increasing warming trend effectively reduces the south to north temperature gradient, thereby diminishing the thermal wind and associated vertical wind shear (Fig. 5). Latitudinal contrasts in upper-level winds further support this interpretation. While the Loess Plateau sits on the "upslope" of the warming trend where gradients are suppressed, the Mongolian Gobi (42°N-48°N) encompasses the peak and the subsequent northward decline of the warming trend. This spatial distribution allows the Mongolian Gobi to maintain a robust meridional gradient, sustaining the dynamical forcing required for strong winds. Consequently, upper-level wind speeds weakened in the mid-latitudes but strengthened over the higher-latitude sector (Fig. S7), contributing to the contrasting evolution of baroclinic instability between regions (Fig. 6).

Since 2020, springtime EGR and near-surface wind speeds have increased over the Mongolian Gobi, with a strong positive correlation between EGR and 10-m wind speed ($r = 0.56$, $p < 0.05$), indicating that enhanced baroclinic instability promotes atmospheric conditions favorable for dust uplift (Fig. S8). However, despite similarly elevated EGR values during 2004, 2010, and 2013, dust occurrence frequency remained relatively low,

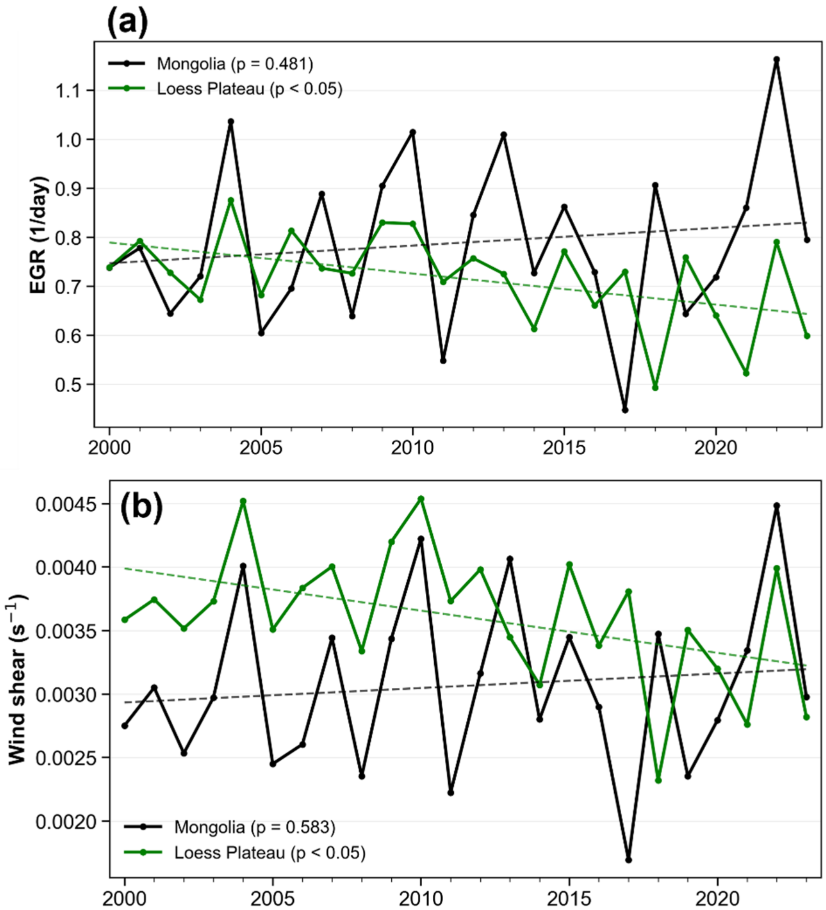

Fig. 4. Time series of March mean (**a**) Eady Growth Rate (EGR) and (**b**) vertical wind shear averaged over the Mongolian Gobi (95–110°E, 42–48°N; black) and Loess Plateau (105–113°E, 34–38°N; green) regions during 2000–2023. Solid lines with markers denote annual regional means, while dashes lines indicate the corresponding linear trends.

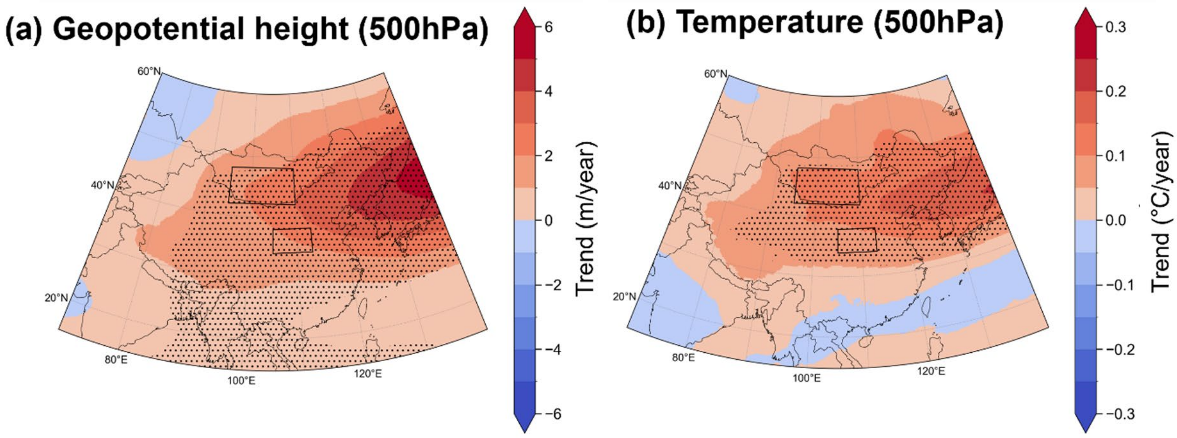

Fig. 5. Spatial distribution of the linear trends in (**a**) 500 hPa geopotential height and (**b**) 500 hPa temperature during March over the period 2000–2023. Dotted areas denote regions where trends are statistically significant at the 90% confidence level ($p < 0.1$). Rectangles mark the Mongolian Gobi and Loess Plateau regions analyzed in this study.

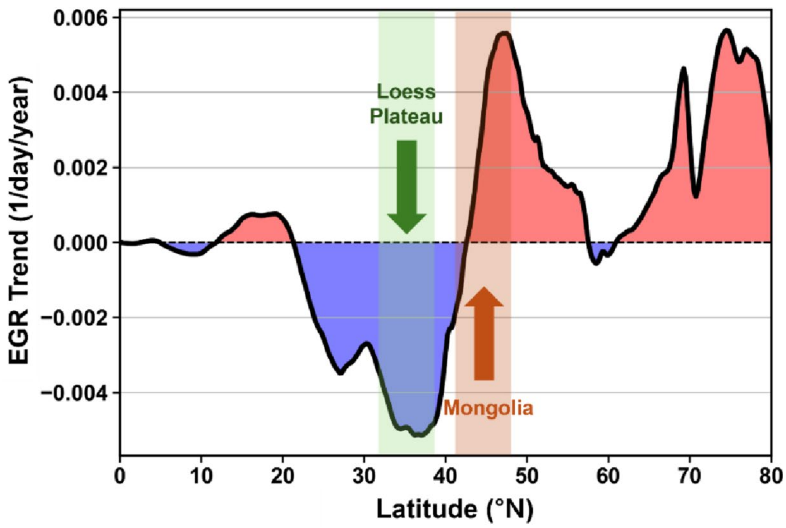

Fig. 6. Latitude-cross section of the linear trend in the Eady Growth rate (EGR), averaged longitudinally over 90–120°E during March for the period 2000–2023. Positive (negative) EGR trends are shaded in red (blue), with the black curve indicating the zonal mean trend profile. The green and brown shaded bands denote the latitude ranges corresponding the Loess Plateau (34–38°N) and the Mongolian Gobi (42–48°N), respectively.

likely owing to the suppressive effects of extensive snow cover and moist soil conditions during those years. This contrast demonstrates that atmospheric instability alone is insufficient to initiate dust activation without concurrent surface drying, highlighting the critical role of land–atmosphere coupling.

Together, snow-cover loss and persistent baroclinic instability explain the recent amplification of dust activation under a compound climate penalty. Snow-cover reduction is therefore a key driver of enhanced March dust activation over the Mongolian Gobi, with warming-induced soil drying and sustained atmospheric instability jointly amplifying dust emissions, particularly since 2020. Unlike other East Asian dust regions, the Mongolian Gobi lacks a mitigating dynamical response, leaving it uniquely vulnerable to intensified dust activation.

This process reflects a broader weakening of the mid-latitude north–south temperature gradient under accelerated warming, which reduces the dynamical forcing for strong upper-level winds. Such a weakening is a robust consequence of Arctic amplification, which preferentially warms high latitudes and erodes the meridional thermal contrast that sustains the mid-latitude jet stream. As a result, baroclinicity and upper-level thermal winds tend to weaken across much of the mid-latitudes, suppressing the atmospheric disturbances that would otherwise promote dust uplift.

However, this weakening is not spatially uniform. Subtropical and lower-latitude warming can enhance upper-tropospheric temperature gradients and wave activity, producing a competing influence that can locally sustain or intensify upper-level winds. The Mongolian Gobi lies near the transition zone of this climatic tug-of-war between Arctic amplification and subtropical warming. In this region, the strengthening influence of subtropical warming offsets the weakening associated with Arctic amplification, allowing vertical wind shear and baroclinic instability to be maintained or even enhanced despite overall mid-latitude warming[28].

This spatially heterogeneous response explains the contrasting evolution of dust-favorable dynamics between the Mongolian Gobi and the Loess Plateau. Over the Loess Plateau, the weakening of the meridional temperature gradient dominates, leading to reduced thermal winds, declining vertical wind shear, and a systematic decrease in baroclinic instability. Over the Mongolian Gobi, by contrast, the competing influence of subtropical warming preserves upper-level flow and sustains baroclinic disturbances, preventing the atmospheric compensation that suppresses dust activation elsewhere.

Consequently, the Mongolian Gobi experiences a fundamentally different dynamical response to climate warming: rather than a weakening of dust-mobilizing winds, the region retains a circulation regime capable of amplifying surface drying into intensified dust emissions. This dynamical asymmetry provides a physically consistent explanation for why the Mongolian Gobi has diverged from broader East Asian dust trends under ongoing climate change. To further refine the physical mechanisms identified in this observational framework, future research utilizing numerical model sensitivity experiments would be beneficial to isolate and quantify the individual contributions of surface and atmospheric drivers under various climate scenarios.

Methods

SYNOP observation data

Dust occurrence frequency was derived from Surface Synoptic Observation present weather observations reported to the World Meteorological Organization (WMO)[29]. We used present weather code 07, which indicates: "Dust or sand raised by wind at or near the station at the time of observation, but no well-developed dust whirl(s) or dust storm observed." Unlike other dust-related weather codes that may include advected or transported dust, code 07 is uniquely suited for detecting local dust emissions at the observation site[30–32].

We utilized SYNOP data from major dust source stations, 15 of which were located in the Mongolian Gobi and 21 stations were situated over the Loess Plateau. March data for the period 2000 to 2023 were analyzed. To ensure data reliability, only stations with at least six observations per day during the month were included in the analysis. For each year, dust frequency was calculated as the ratio of the number of code 07 reports to the total number of available observations at each site. This method allowed for a consistent, spatially and temporally comparable assessment of local dust activation.

ERA5 reanalysis data

To assess the thermal and dynamic atmospheric conditions associated with dust activation, we used ERA5 reanalysis data produced by the European Centre for Medium-Range Weather Forecasts (ECMWF). ERA5 provides hourly global atmospheric data at a spatial resolution of approximately 0.25° (~ 31 km), with consistent assimilation of satellite, in situ, and upper-air observations[33,34]. From this dataset, we used 2-m air temperature, 10-m wind speed, soil temperature, and volumetric soil water content to evaluate the surface conditions that influence dust emissions.

Additionally, atmospheric baroclinic instability was assessed using the Eady Growth Rate (EGR), a commonly used diagnostic in mid-latitude meteorology that incorporates vertical wind shear and static stability. The EGR quantifies the potential for the development of synoptic-scale disturbances and is expressed as

$$EGR = 0.31 \times \frac{f}{N} \times \frac{dV}{dZ}$$

where f is the Coriolis parameter, dV/dz is the vertical wind shear between two pressure levels and N is the Brunt-Vaisala frequency representing static stability.

In this study, EGR was calculated using zonal and meridional wind components at 850 and 500 hPa, capturing the vertical shear across the lower troposphere, where baroclinic development is most active. Temperature and geopotential height data at these levels were also used to calculate static stability. All variables were spatially averaged over each study region to represent region-scale environmental conditions.

Terra-MODIS snow cover data

Snow cover data were obtained from the Terra Moderate Resolution Imaging Spectroradiometer, which provides the daily snow cover fraction at a spatial resolution of 0.05°. We used the MOD10C1 Version 6.1 product, which includes cloud-masked global snow cover estimates based on Normalized Difference Snow Index (NDSI) thresholds and spectral reflectance. Snow cover percentages were spatially averaged over the Mongolian Gobi to represent the regional-scale snow conditions relevant to dust activation. For quality assurance, only pixels flagged as "snow" and free from cloud contamination were included in the analysis. Detailed algorithm information is available in the official MODIS user guide[35].

Data availability

The ERA5 reanalysis data are available from Copernicus Climate data store (surface: DOI: [10.24381/cds.f17050d7](https:/doi.org/10.24381/cds.f17050d7), vertical: DOI: [10.24381/cds.6860a573] (https:/doi.org/10.24381/cds.6860a573)), and SYNOP observation data are available from Korea Meteorological Administration ([https://apihub.kma.go.kr/](https:/apihub.kma.go.kr)). MODIS snow cover data is accessible from the NASA National Snow and Ice Data Center Distributed active archive center ([https://doi.org/10.5067/MODIS/MOD10CM.061](https:/doi.org/10.5067/MODIS/MOD10CM.061)).

Received: 10 January 2026; Accepted: 21 April 2026
Published online: 16 June 2026

References

1. Middleton, N. J. Desert dust hazards: A global review. *Aeolian Res.* **24**, 53–63. https://doi.org/10.1016/j.aeolia.2016.12.001 (2017).
2. Han, J., Dai, H. & Gu, Z. L. Sandstorms and desertification in Mongolia, an example of future climate events: a review. *Environ. Chem. Lett.* **19**, 4063–4073. https://doi.org/10.1007/s10311-021-01285-w (2021).
3. Uno, I. et al. Large Asian dust layers continuously reached North America in April 2010. *Atmos. Chem. Phys.* **11**, 7333–7341. https://doi.org/10.5194/acp-11-7333-2011 (2011).
4. Ahmadzai, H., Malhotra, A. & Tutundjian, S. Assessing the impact of sand and dust storm on agriculture: Empirical evidence from Mongolia. Plos One 18 (2023). https://doi.org:ARTN e026927110.1371/journal.pone.0269271.
5. Hong, Y. C. et al. Asian Dust Storm and pulmonary function of school children in Seoul. *Sci. Total Environ.* **408**, 754–759. https://doi.org/10.1016/j.scitotenv.2009.11.015 (2010).
6. An, L. C. et al. Temporal and spatial variations in sand and dust storm events in East Asia from 2007 to 2016: Relationships with surface conditions and climate change. *Sci. Total Environ.* **633**, 452–462. https://doi.org/10.1016/j.scitotenv.2018.03.068 (2018).
7. Wu, C. L., Lin, Z. H., Shao, Y. P., Liu, X. H. & Li, Y. Drivers of recent decline in dust activity over East Asia. Nat Commun 13 (2022). https://doi.org:ARTN 710510.1038/s41467-022-34823-3.
8. Tai, A. P. K. et al. Impacts of climate and land cover variability and trends on springtime East Asian dust emission over 1982–2010: A modeling study. Atmos Environ 254 (2021). https://doi.org:ARTN 11834810.1016/j.atmosenv.2021.118348.
9. Zhou, W. C., Wang, H. J. & Ge, Q. S. Contributions of climatic factors and vegetation cover to the temporal shift in Asian dust events. Npj Clim Atmos Sci 7 (2024). https://doi.org:ARTN 32810.1038/s41612-024-00887-9.
10. He, Y. et al. Mega Asian dust event over China on 27–31 March 2021 observed with space-borne instruments and ground-based polarization lidar. Atmos Environ 285 (2022). https://doi.org:ARTN 11923810.1016/j.atmosenv.2022.119238.
11. Liang, P. et al. Revealing the dust transport processes of the 2021 mega dust storm event in northern China. *Sci. Bull.* **67**, 21–24. https://doi.org/10.1016/j.scib.2021.08.014 (2022).
12. Jin, J. B. et al. Inverse modeling of the 2021 spring super dust storms in East Asia. *Atmos. Chem. Phys.* **22**, 6393–6410. https://doi.org/10.5194/acp-22-6393-2022 (2022).
13. Zhang, Y., Chen, Y., Chen, S. Y., Alam, K. & Chen, J. Y. Mongolia dust transport across borders under the background of global warming. Global Planet Change 239 (2024). https://doi.org:ARTN 10450910.1016/j.gloplacha.2024.104509.
14. Davi, N. K. et al. Accelerated Recent Warming and Temperature Variability Over the Past Eight Centuries in the Central Asian Altai From Blue Intensity in Tree Rings. *Geophys. Res. Lett.* **48** https://doi.org:ARTN (2021). e2021GL09293310.1029/2021GL092933.
15. Liu, L. et al. Climate factors influencing springtime dust activities over Northern East Asia in 2021 and 2023. Atmos Res 303 (2024). https://doi.org:ARTN 10734210.1016/j.atmosres.2024.107342.
16. Jeon, J. G., Yeh, S. W. & Song, S. Y. Changes in the hydrological properties of inner East Asia during the boreal summer and possible mechanisms. *Clim. Dynam.* **62**, 6745–6755. https://doi.org/10.1007/s00382-024-07234-x (2024).
17. Huang, J. et al. Dryland climate change: Recent progress and challenges. *Rev. Geophys.* **55**, 719–778. https://doi.org/10.1002/2016rg000550 (2017).
18. Zhang, X. et al. Quantifying the Effects of Snow on the Beginning of Vegetation Growth in the Mongolian Plateau. Remote Sens-Basel 15 (2023). https://doi.org:ARTN 124510.3390/rs15051245.
19. Zhu, Q. Z. & Liu, Y. Z. The dominant factor in extreme dust events over the Gobi Desert is shifting from extreme winds to extreme droughts. Npj Clim Atmos Sci 7 (2024). https://doi.org:ARTN 14110.1038/s41612-024-00689-z.
20. A tug-of-war over the mid-latitudes. Nat Commun 10. (2019). https://doi.org:ARTN 557810.1038/s41467-019-13714-0.
21. Hsu, P. C., Hsu, H. H., Hong, H. J. & Chen, Y. T. Subtropical warming enhances North Pacific midlatitude winter storm track activity in recent decades. Npj Clim Atmos Sci 8 (2025). https://doi.org:ARTN 23510.1038/s41612-025-01108-7.
22. Cai, Q. Y. et al. Recent pronounced warming on the Mongolian Plateau boosted by internal climate variability. *Nat. Geosci.* **17** https://doi.org/10.1038/s41561-024-01377-6 (2024).
23. Li, D. S. et al. Revisiting snowmelt dynamics and its impact on soil moisture and vegetation in mid-high latitude watershed over four decades. Agr Forest Meteorol 362 (2025). https://doi.org:ARTN> 11035310.1016/j.agrformet.2024.110353.
24. Kurosaki, Y. & Mikami, M. Threshold wind speed for dust emission in east Asia and its seasonal variations. J Geophys Res-Atmos 112 (2007). https://doi.org:ARTN D1720210.1029/2006jd007988.
25. Kimura, R. & Shinoda, M. Spatial distribution of threshold wind speeds for dust outbreaks in northeast Asia. *Geomorphology* **114**, 319–325. https://doi.org/10.1016/j.geomorph.2009.07.014 (2010).
26. Foroutan, H. & Pleim, J. E. Improving the simulation of convective dust storms in regional-to-global models. *J. Adv. Model. Earth Sy.* **9**, 2046–2060. https://doi.org/10.1002/2017ms000953 (2017).
27. Lindzen, R. S. & Farrell, B. A. Simple Approximate Result for the Maximum Growth-Rate of Baroclinic Instabilities. *J. Atmos. Sci.* **37**, 1648–1654 (1980). – 0469(1980)037 < 1648:Asarft > 2.0.Co;2https://doi.org:Doi 10.1175/1520.
28. Mao, R., Ho, C. H., Shao, Y. P., Gong, D. Y. & Kim, J. Influence of Arctic Oscillation on dust activity over northeast Asia. *Atmos. Environ.* **45**, 326–337. https://doi.org/10.1016/j.atmosenv.2010.10.020 (2011).
29. (WMO) World Meteorological Organization *Guide to Instruments and Methods of Observation (WMO-No.8), Volume I* (Geneva, 2024).
30. Lee, W. J. & Kang, M. S. A Study on the Updating of Asian Dust Source Regions in Asian Dust Aerosol Model Version3 (ADAM3) in KMA. *J. Korean Soc. Atmos. Environ.* **39**, 294–307 (2023).
31. Lee, J. J. & Kim, C. H. Roles of surface wind, NDVI, and snow cover in recent changes in Asian dust storm occurrence frequency. *Atmos. Environ.* **59**, 366–375 (2012).
32. Shao, Y. & Dong, C. H. A review on East Asian dust storm climate, modelling and monitoring. *Globe Planet. Change.* **52**, 1–22 (2006).
33. Hersbach, H. et al. : ERA5 monthly averaged data on single levels from 1940 to present. Copernicus Climate Change Service (C3S) Climate Data Store (CDS), (2023). https://doi.org/10.24381/cds.f17050d7
34. Hersbach, H. et al. : ERA5 monthly averaged data on pressure levels from 1940 to present. Copernicus Climate Change Service (C3S) Climate Data Store (CDS), (2023). https://doi.org/10.24381/cds.6860a573
35. Hall, D. K. & Riggs, G. A. MODIS/Terra Snow Cover Monthly L3 Global 0.05° CMG, Version 61. NASA National Snow and Ice Data Center Distributed Active Archive Center, Boulder, CO, USA. (2021). https://doi.org/10.5067/MODIS/MOD10CM.061

Author contributions

S.-S.O. and H.-J.L. perfomred the experiments. C.-H.K. conceived and designed the research. S.-S.O., H.B., H.-J.L. and H.-Y.J. analysed the data and interpreted the results. S.-S.O wrote the paper. All authors discussed the results and commented on the manuscript.

Funding
This work was supported by the Basic Science Research Program through the National Research Foundation of Korea (NRF), funded by the Ministry of Education [RS-2020-NR049592] and [RS-2020-NR054792].

Declarations

Competing interests
The authors declare no competing interests.

Additional information
Supplementary Information The online version contains supplementary material available at https://doi.org/10.1038/s41598-026-50408-2.

Correspondence and requests for materials should be addressed to H.-J.L. or C.-H.K.

Reprints and permissions information is available at www.nature.com/reprints.